SUPPLEMENTAL FIGURES

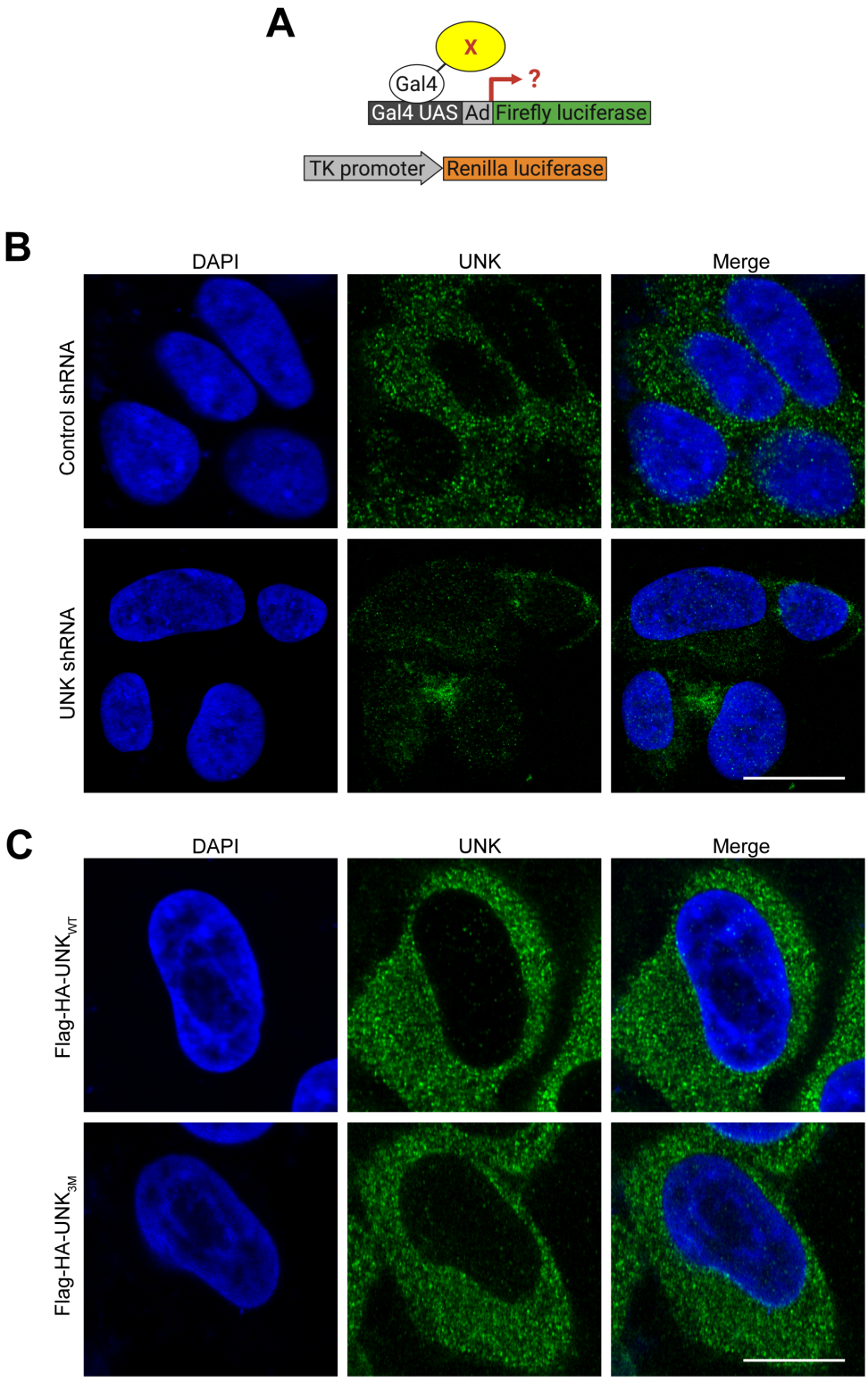

Figure S1. Transcriptional activity and intracellular localization of Unkempt, related to Figures 1 and 2.

(A) Principle of a dual luciferase reporter assay used to detect transcriptional activity of UNK. A tested protein (X) is tagged with the Gal4 DNA-binding domain for recruitment via Gal4 upstream activating sequences (Gal4 UAS) to the adenovirus major late promoter (Ad) driving minimal expression of the firefly luciferase reporter gene. The thymidine kinase (TK) promoter-driven Renilla luciferase serves as an internal control (Methods).
(B) Endogenous UNK detected by immunofluorescence using UNK-specific antibody in SH-SY5Y human neuroblastoma cells stably expressing either shRNA targeting luciferase (Control shRNA, top) or UNK (bottom). Scale bar, 10 μm.
(C) Ectopic Flag-HA-tagged UNK_{WT} or UNK_{3M} (D) detected by immunofluorescence using an HA-specific antibody in inducible HeLa cells treated with doxycycline for 24 h. Scale bar, 10 μm.
DAPI was used to visualize nuclei. Confocal images shown in (B) and (C) are representative of $n \geq 3$ experiments.

A

Gene Symbol	MW (kDa)	Total peptide count			
		uninduced	WT	3M	dPAM2
CNOT1	266.77	0	80	0	54
CNOT10	82.26	0	9	0	3
CNOT3	81.82	0	6	0	3
CNOT7	32.72	0	5	0	6
CNOT2	59.7	0	4	0	6
CNOT11	55.18	0	2	0	2
CNOT8	33.52	0	2	0	0
CNOT9	33.61	0	2	0	1
PABPC1	70.63	4	127	105	0
PABPC4	70.74	0	45	32	0

B

```
LIG_PAM2_1: ..[LFP][NS][PIVTAFL].A..(([FY].[PYLF])|(W..)).

                          495        506
                           |          |
     H.sapiens  UNKEMPT    PGMNANALPFYP
     M.musculus Unkempt    PGMNANALPFYP
     H.sapiens  PAIP1      SKLSVNAPEFYP
     H.sapiens  PAIP2      SNLNPNAKEFVP
                           . :. **  * *
```

C

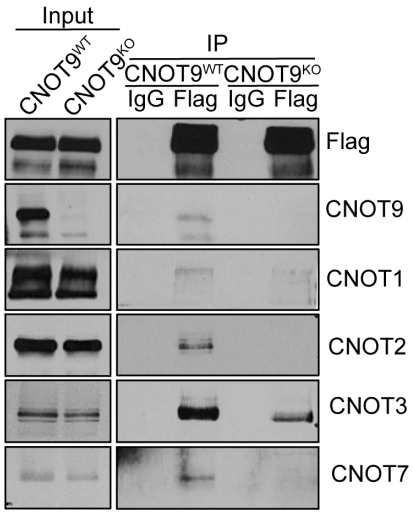

Figure S2. Analyses of interactions between Unkempt and its effectors, related to Figure 3.
(A) Total peptide counts detected by mass spectrometry analysis of tandem affinity-purified protein complexes prepared from uninduced (mock) or UNK_{WT}, UNK_{3M}, or UNK_{dPAM2} - expressing cells (Methods).
(B) Identification of the PAM2-like motif in UNK. A search for either of the two PAM2 motifs annotated in the ELM database (LIG_PAM2_1 and LIG_PAM2_2; http://elm.eu.org/) identified a 12-residue PAM2-like peptide sequence that deviates from the canonical LIG_PAM2_1 motif (regular expression shown on top) at one position, highlighted in red. PAM2 motifs of PABP-interacting proteins 1 and 2 (PAIP1 and PAIP2) are shown for comparison[41,86].

(C) Co-IP of endogenous CCR4-NOT subunits with Flag-HA-tagged UNK_{WT} from *CNOT9*^{WT} or *CNOT9*^{KO} HeLa cells. Precipitated proteins were detected by western blot analysis using the indicated antibodies (n = 2).

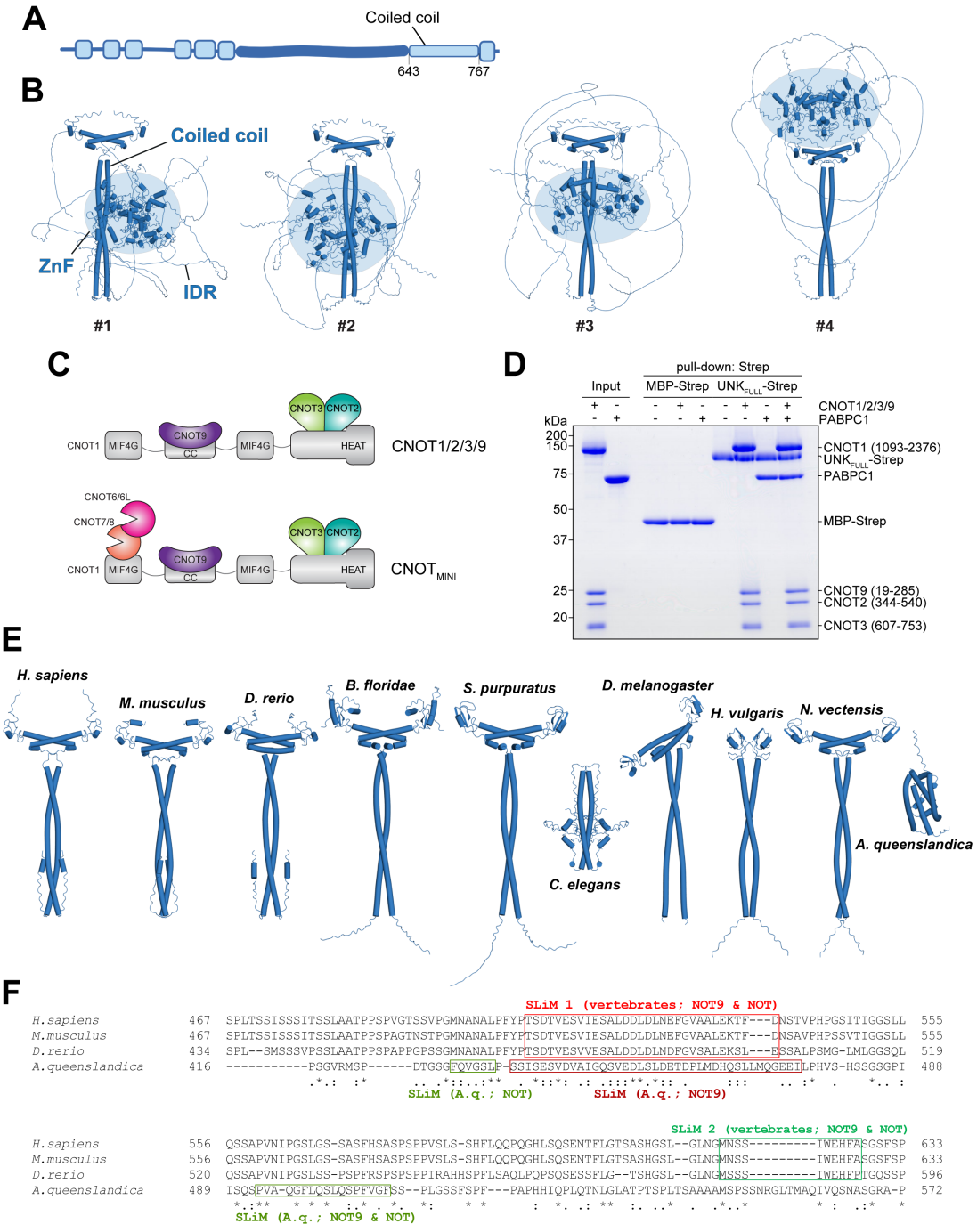

Figure S3. Structural and functional insights into the Unkempt-effector interface, related to Figures 4 and 5.
(A) Map of UNK protein indicating the location of the predicted coiled coil.
(B) Four AlphaFold predictions of the homodimer full-length mouse UNK protein showing the central coiled coil stabilizing the dimer with the positioning of the zinc fingers (ZnF, blue sphere) and the unstructured IDR being entirely stochastic with respect to the coil.
(C) Schematic representation of the reconstituted CNOT1/2/3/9 (top) and CCR4-NOT$_{MINI}$ (bottom) complexes. The rationale for using the larger, six-subunit CCR4-NOT$_{MINI}$ complex instead of CNOT1/2/3/9 for the mass photometry experiment shown in Figure 5D was to avoid signal overlap (the molecular weight of CNOT1/2/3/9 is similar to UNK dimer).

(D) Coomassie-stained polyacrylamide gel of an in vitro pull-down assay with MBP-Strep alone or recombinant UNK_{FULL}-Strep after incubation with PABPC1 and/or CNOT1/2/3/9, as indicated (n = 3).
(E) A representative AlphaFold prediction of the UNK coiled coil homodimer for each of the shown UNK orthologs (*Homo sapiens*, human; *Mus musculus*, house mouse; *Danio rerio*, zebrafish; *Branchiostoma floridae*, Florida lancelet; *Stronglycentrotus purpuratus*, sea urchin; *Caenorhabditis elegans*, roundworm; *Drosophila melanogaster*, fruit fly; *Hydra vulgaris*, fresh-water polyp; *Nematostella vectensis*, starlet sea anemone; *Amphimedon queenslandica*, sponge). See also Figure 5A.
(F) Sequence alignment of IDRs of the indicated UNK orthologs. Locations of SLiMs in contact with CCR4-NOT, as predicted by AlphaFold, are highlighted with red (matching SLiM 1 in mouse UNK) and green (matching SLiM 2 in mouse UNK) rectangles separately for vertebrates and *A. queenslandica* (*A.q.*), which harbors the evolutionarily most distant known UNK ortholog[17,54]. "NOT9" or "NOT" indicates that the SLiM is predicted to only contact one specific region in the respective module and "NOT9 & NOT" indicates repeated SLiM use.

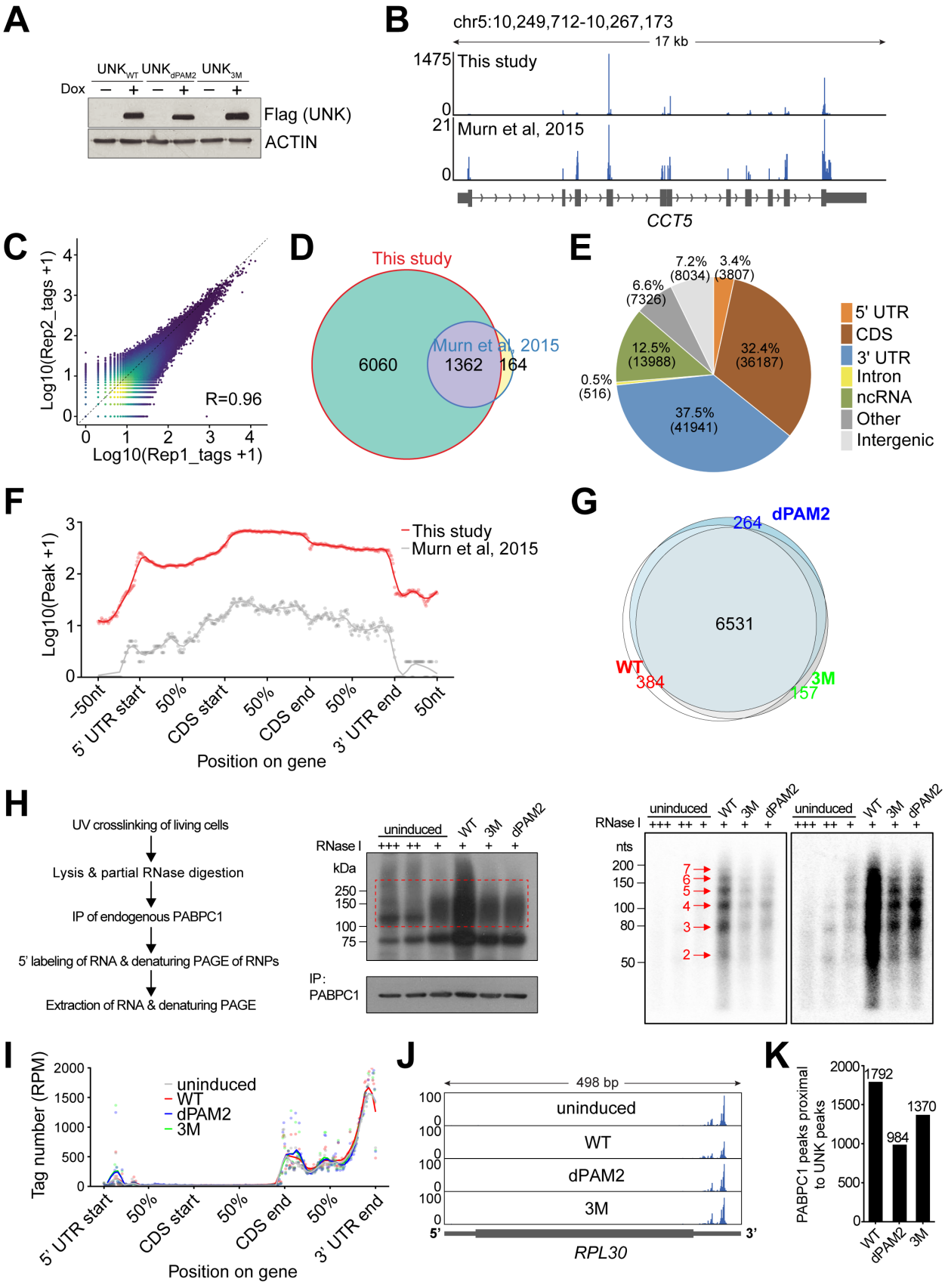

Figure S4. RNA binding by UNK$_{WT}$, UNK$_{3M}$, UNK$_{dPAM2}$, and PABPC1, related to Figure 6.

(A) Western blot analysis of HeLa cells inducibly expressing Flag-HA-tagged UNK$_{WT}$, UNK$_{3M}$, or UNK$_{dPAM2}$ at 24 hours of treatment with Dox (n = 4).

(B) Genome browser view of the *CCT5* gene locus visualizing reproducibility of UNK$_{WT}$ crosslink events between iCLIP replicates of this (top) and a previous (bottom) study[16].

(C) Density scatterplot comparing crosslink events per peak between replicates 1 and 2 of the UNK$_{WT}$ iCLIP experiment. UNK$_{3M}$ and UNK$_{dPAM2}$ showed similar levels of reproducibility among iCLIP replicates (data now shown).

(D) Comparison of mRNA targets of UNK$_{WT}$ in HeLa cells identified by iCLIP in this study and those reported previously[16].

(E) Distribution of UNK$_{WT}$ iCLIP peaks among different RNA biotypes and mRNA segments determined in this study.

(F) Metatranscript analyses of the current (red) and previously reported (gray) iCLIP datasets showing the positional frequency of UNK$_{WT}$ binding sites on mRNAs[16].

(G) Comparison of mRNA targets of UNK$_{WT}$, UNK$_{3M}$, and UNK$_{dPAM2}$ identified by iCLIP. n = 4 iCLIP replicates were performed for each condition. See also Table S2 and Methods.

(H) Analysis of bulk interactions of PABPC1 with poly(A) tails. Labeled, partially RNase-digested PABPC1-bound RNA was extracted from cells expressing or not UNK$_{WT}$, UNK$_{3M}$, or UNK$_{dPAM2}$ as outlined in the protocol on the left. Middle panels show autoradiogram of labeled PABPC1 RNP complexes (top) and the corresponding western blot of immunoprecipitated PABPC1 (bottom). Red dashed frame demarcates the area from which RNA was extracted. Two autoradiograms on the right are different exposures of the extracted RNA after resolution by denaturing PAGE. Red arrows point to footprints of 27-nt oligomers (red numbers) protected from RNase, matching the pattern of serial binding of PABPC1 to poly(A) tails[24,41]. Note that the periodic footprint pattern of PABPC1 is not perturbed by expression of UNK but is sensitive to the concentration of RNase I (plus signs) (n = 4).

(I)-(K) iCLIP analysis of PABPC1-RNA interactions.

(I) Proportional metatranscript analysis of iCLIP data showing the positional frequency of crosslink events for PABPC1 on different segments of mRNA in cells expressing UNK$_{WT}$, UNK$_{3M}$, or UNK$_{dPAM2}$, or in uninduced cells. Data points represent normalized crosslink events summarized over every percent of a given mRNA segment. CDS, coding sequence.

(J) Mapping PABPC1 iCLIP data onto UNK target transcripts. iCLIP data from four replicates were summed, normalized, and mapped to *RPL30* mRNA.

(K) Occurrence of PABPC1 iCLIP peaks in the vicinity (+/- 20 nts) of UNK$_{WT}$, UNK$_{dPAM2}$, or UNK$_{3M}$ iCLIP peaks on mRNA. Note the reduction in the number of observed neighboring peaks upon disrupting UNK–PABPC interactions (UNK$_{dPAM2}$) and a weaker similar effect upon disrupting UNK–CCR4-NOT interactions (UNK$_{3M}$). See also Figure 6F.

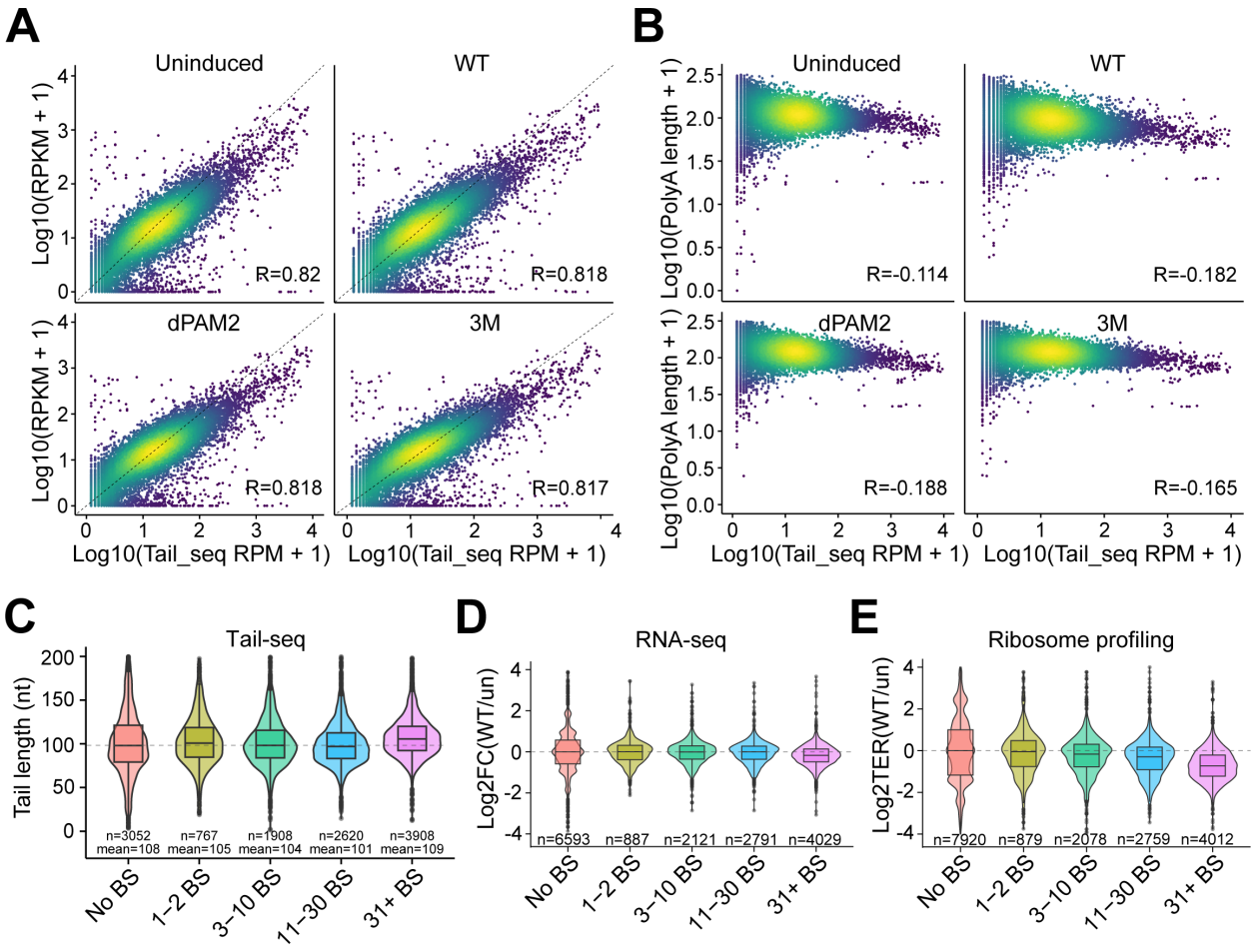

Figure S5. Impact of Unkempt on mRNA poly(A) tail length. Related to Figure 7.
(A) Scatterplots comparing log10-scaled transcript abundance determined by mRNA-seq (RPKM + 1) and Tail-seq (RPM + 1) analyses of each indicated sample, showing high correlation (n = 2).
(B) Scatterplots comparing log10-scaled transcript abundance (RPM + 1) and poly(A) tail length (value + 1), both determined by Tail-seq. Note the slight and expected tendency of highly expressed mRNAs to have relatively short poly(A) tails[43-45] (n = 2).
(C) Comparison of average poly(A) tail lengths of transcripts binned into groups according to the number of UNK binding sites (BS) per transcript. Data are shown for UNK_{WT}-expressing cells. Similar, minimal changes were observed for uninduced cells and cells expressing UNK_{3M} or UNK_{dPAM2} (data now shown). Numbers of transcripts (n) and mean lengths of their poly(A) tails are indicated for each group of transcripts (n = 2).
(D) RNA-seq results for transcripts binned into groups as in (C), showing changes in steady-state mRNA levels between UNK_{WT}-expressing and uninduced cells (un; n = 3). See also Figures 7A and 7D.
(E) Ribosome profiling data for transcripts binned into groups as in (C), showing changes in ribosome occupancy between UNK_{WT}-expressing and uninduced cells (un; n = 2). See also Figures 7E and 7H.

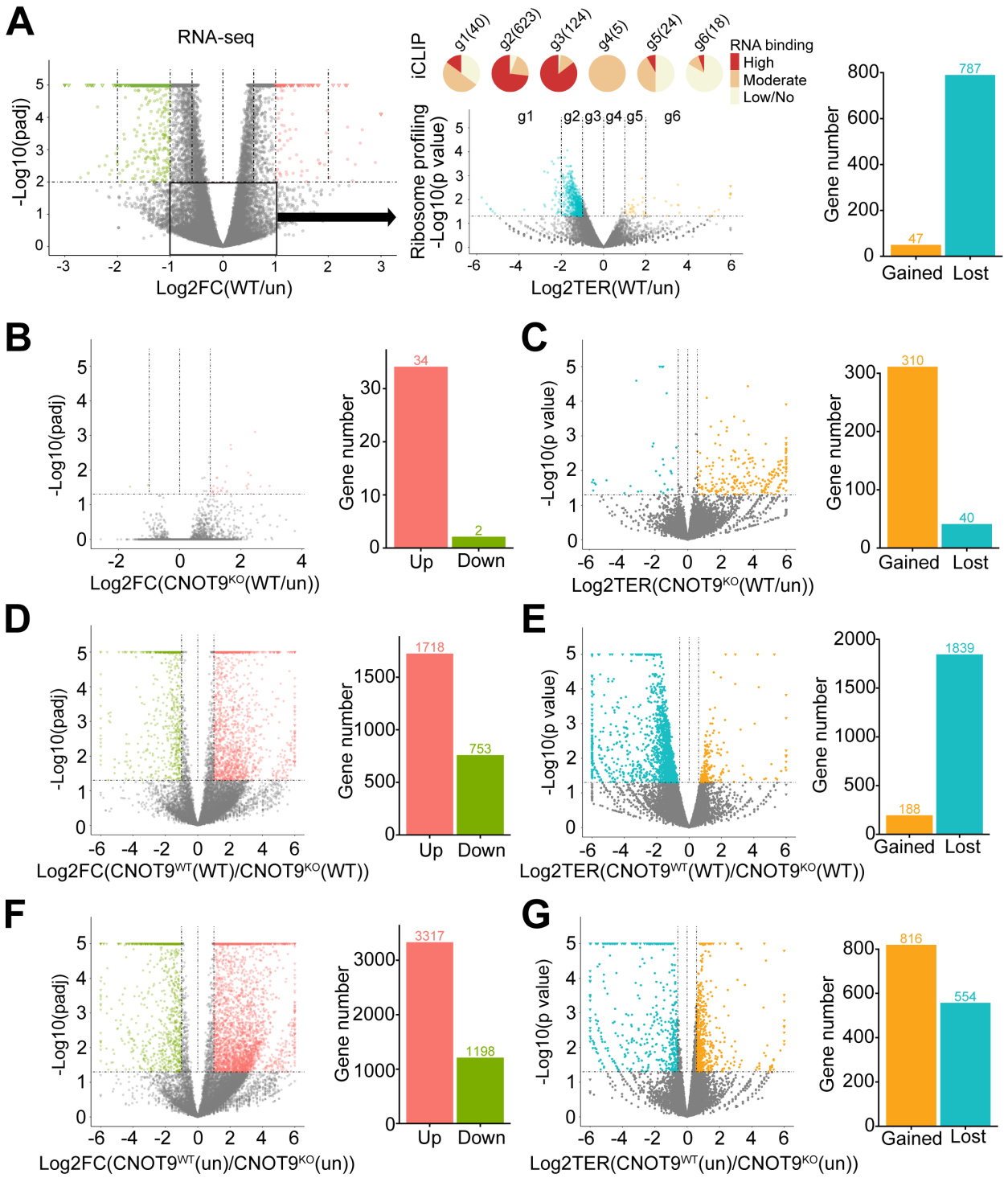

Figure S6. Reduced translational efficiency mediated by Unkempt. Related to Figure 7.
(A) Translational repression of mRNAs that show little change in abundance upon expression of UNK. mRNAs with small (< 2-fold) and insignificant (adjusted p > 0.01) changes in steady-state levels comparing UNK_{WT}-expressing to uninduced cells (group of mRNAs indicated by a black frame in the left plot) were analyzed for changes in ribosome occupancy (middle plot). Pie charts above the middle plot show RNA-binding information and transcript numbers in

each group of significantly regulated transcripts (g1-g6), as in Figures 7E-7G. Bar chart on the right indicates total numbers of transcripts with gained or lost ribosome occupancy ($p < 0.05$) ($n = 2$). See also Figures 7A, 7E, and 7H. (B)-(G) Reliance of translational repression by UNK on CNOT9. Three pairs of samples are compared by RNA-seq and ribosome profiling to document this reliance as well as the effect of CNOT9 alone: (B, C) CNOT9 KO cells ($CNOT9^{KO}$) expressing or not UNK_{WT}, (D, E) uninduced (un) CNOT9 WT ($CNOT9^{WT}$) and $CNOT9^{KO}$ cells, and (F, G) CNOT9 WT and CNOT9 KO cells expressing UNK_{WT}. Significantly regulated transcripts with twofold or larger changes in abundance (RNA-seq) or ribosome occupancy (ribosome profiling) are highlighted in color. Bar charts in panels (C), (E), and (G) indicate total numbers of transcripts with gained or lost ribosome occupancy ($p < 0.05$). ($n = 3$ for RNA-seq; $n = 2$ for ribosome profiling).

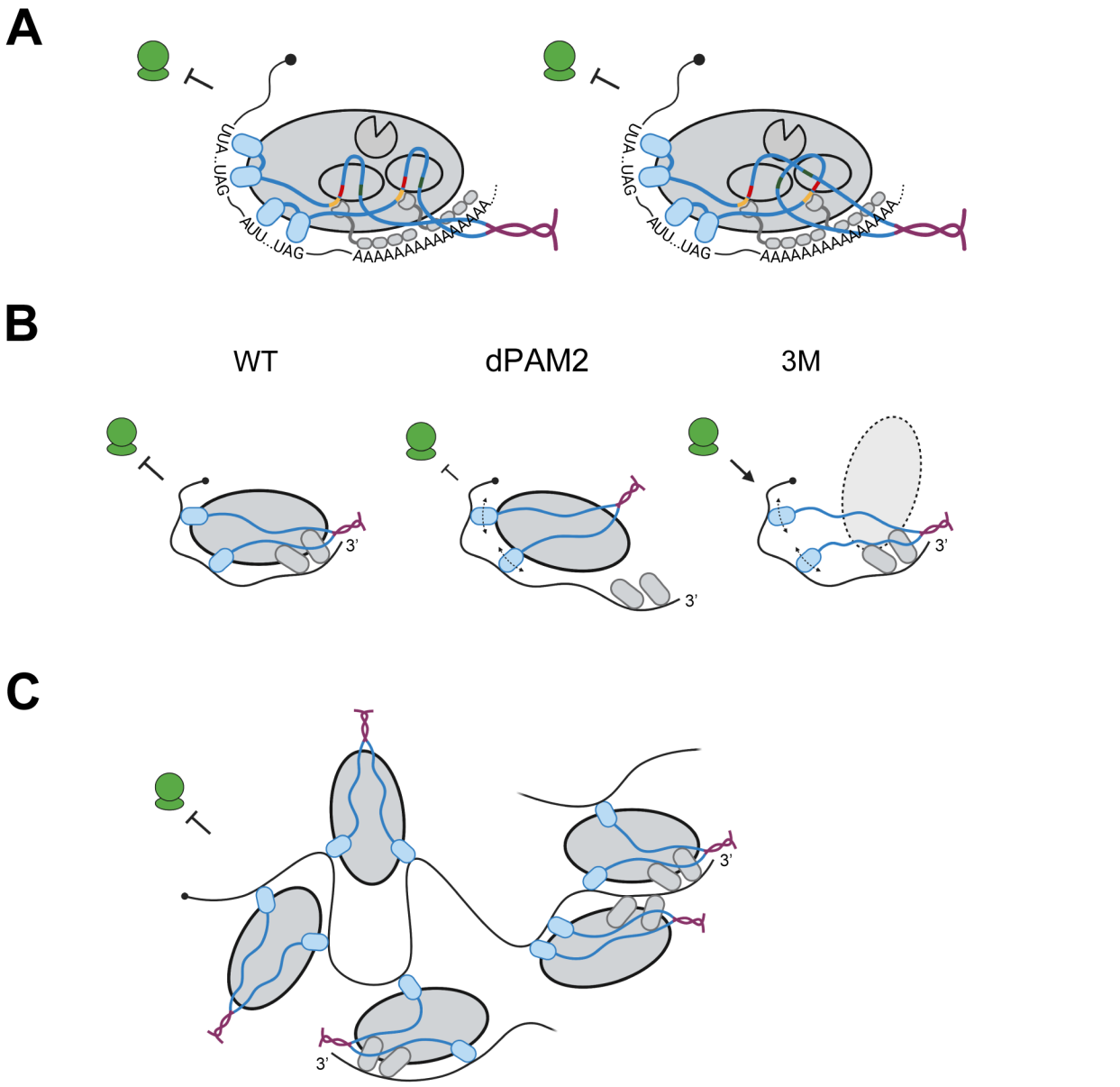

Figure S7. PABPC1-RNA interactions and models of Unkempt-effector interface. Related to Figure 7.
(A)-(C) Models of UNK-effector interface.
(A) Two possible modes of interaction between the IDR-embedded SLiMs of UNK and the NOT9 and NOT modules of CCR4-NOT. See also Figure 7J.
(B) Models illustrating how disrupting the interactions between UNK and PABPC (UNK_{dPAM2}) or CCR4-NOT (UNK_{3M}) might affect RNP organization and function. Curved dashed lines with arrowheads on each end indicate compromised RNA sequence recognition by UNK. Inhibitory arrows pointing to the ribosome (green shapes) or the arrow pointing to the RNP indicate translational repression or lack thereof, respectively.
(C) A larger RNP particle formed via association of multiple copies of the UNK dimer–CCR4-NOT–PABPC complex with mRNA.

SUPPLEMENTAL TABLES

Table S1. List of UNK mutants used in this study.

Table S2. iCLIP targets of UNK_{WT}, UNK_{3M}, and UNK_{dPAM2} in HeLa cells.

Table S3. PABPC1 iCLIP targets in uninduced HeLa cells and in HeLa cells expressing UNK_{WT}, UNK_{3M}, or UNK_{dPAM2}.

Table S4. RNA-seq analyses of uninduced HeLa cells and of HeLa cells expressing UNK_{WT}, UNK_{3M}, or UNK_{dPAM2}.

Table S5. Poly(A) tail length analyses of uninduced HeLa cells and of HeLa cells expressing UNK_{WT}, UNK_{3M}, or UNK_{dPAM2}.

Table S6. Ribosome profiling analyses of uninduced HeLa cells and of HeLa cells expressing UNK_{WT}, UNK_{3M}, or UNK_{dPAM2}.